Hydrological Processes

WILEY

RESEARCH ARTICLE OPEN ACCESS

Understanding Fire Skips in Juvenile Pine Plantations: Exploring the Relationship Between Fuel Moisture Content and Burn Severity

R. Xiao[1] | J. M. Shea[2] | V. Foord[3] | P. J. Burton[4]

[1]Department of Geography and Environmental Management, University of Waterloo, Waterloo, Ontario, Canada | [2]Department of Geography, Earth, and Environmental Science, University of Northern British Columbia, Prince George, British Columbia, Canada | [3]British Columbia Ministry of Forests, Prince George, British Columbia, Canada | [4]Department of Ecosystem Science and Management, University of Northern British Columbia, Terrace, British Columbia, Canada

Correspondence: J. M. Shea (joseph.shea@unbc.ca)

Received: 2 June 2025 | **Revised:** 25 September 2025 | **Accepted:** 5 October 2025

Funding: This work was supported by the Ministry of Forests, Government of British Columbia, Natural Resources Canada in the program Emergency Management Strategy Program, National Science and Engineering Research Council.

Keywords: burn severity | fire refugia | fuel moisture content | remote sensing | wildfire

ABSTRACT

Wildfires are increasing in size and severity due to climate change, and pose a serious threat to humans, infrastructure, and industry. In western North America, wildfires often leave unburned blocks of forest known as fire skips, fire islands, or fire refugia. Research elsewhere has suggested that young forests burn more severely, while mature forest is often found unburned as wildfire refugia. However, preliminary observations in central British Columbia suggest that some planted juvenile stands burn less severely than the surrounding mature forests. The existence of these fire skips could be due to differences in fuel moisture content (FMC), stand structure characteristics that influence fire spread, or both. To identify the role of FMC in fire skips, this study develops relationships between 6116 individual ground-based FMC measurements and remote sensing data collected in 2021 and 2022. Remotely sensed estimates of pre-fire FMC were then used to analyse burn severities in different stand types encountered in three major wildfires in central British Columbia in 2017 and 2018. Juvenile plantations, mostly dominated by lodgepole pine (*Pinus contorta var. latifolia*), had lower burn severity than mature and recent cutblocks (open sites) in three case study areas. No significant relationships were found between pre-fire satellite-estimated FMC and burn severity in mature forest and juvenile plantations. However, at open stands, moderate correlations between estimated duff FMC and difference normalized burn ratio (dNBR) were found in two case study areas. This work provides tools for assessing pre-fire FMC at large spatial scales and suggests that the limited fire severity in juvenile stands may be a function of stand characteristics other than pre-fire FMC.

1 | Introduction

Wildfires threaten humans, infrastructure, and industry (McGee et al. 2015), and with the impact of climate change, they are anticipated to become more frequent and severe (Flannigan et al. 2000; Parisien et al. 2023). In western North America, wildfires often leave patches of unburned forest known as fire skips, fire islands, or fire refugia (Krawchuk et al. 2016). While industrially planted forests in southwestern Oregon, USA, have been shown to burn at high severities compared to natural forests (Zald and Dunn 2018), initial observations from central British Columbia (BC) suggest a more complex pattern, with some young forests burning less severely than mature forests (Burton et al. 2019). This raises the question of whether stand

This is an open access article under the terms of the Creative Commons Attribution License, which permits use, distribution and reproduction in any medium, provided the original work is properly cited.

© 2025 The Author(s). *Hydrological Processes* published by John Wiley & Sons Ltd.

structure and fuel characteristics may influence burn severity differently across forest types.

Fuel moisture content (FMC) plays a key role in wildfire susceptibility and behaviour (Scott and Burgan 2005; Krawchuk et al. 2009). In central BC, both replanted young stands and naturally regenerating stands are typically dense and uniform, often dominated by lodgepole pine (*Pinus contorta var. latifolia*; Wang et al. 2019; Burton 2023). These structural conditions may support higher in-stand humidity, lower temperatures and lower wind speeds, and thus higher fuel moisture (Burton 2023). However, it is unclear if FMC actually varies significantly between juvenile plantations and mature or old forests in the same locality. To address this gap, this study first examines FMC differences across stand types using field observations, then develops statistical relationships between FMC and remote sensing indices, and finally applies these to wildfire cases in central BC.

Field observations of FMC provide accurate information on a key fire risk factor but are time-intensive, represent only a specific point in space and time, and may miss rapid fluctuations in FMC (Caccamo et al. 2011). Since wildfires often ignite in duff and fine woody debris in the forest understory (Ryan 2002; Norum and Miller 1984; Hartford and Frandsen 1992), the moisture of these fuels strongly affects ignition probability (Dennison et al. 2008; Chuvieco et al. 2009; Nolan et al. 2016). Low FMC is typically required for wildfire initiation and spread, making the estimation of FMC and its variability critical for fire risk assessment and prevention (Dennison et al. 2008; Yebra et al. 2013). Thus, linking FMC dynamics to broader landscape-scale patterns can be useful for improving wildfire susceptibility.

Remotely-sensed spectral reflectance provides a practical way to monitor FMC across space and time. These methods rely on differences in spectral signatures of healthy versus stressed vegetation (Ceccato et al. 2002) and have been used to estimate FMC in both broadleaf (Danson and Bowyer 2004) and coniferous foliage (Qi et al. 2014). Remote sensing has also been widely used to map burn severity in historical fires (Parks et al. 2014). Connecting remote sensing data with ground-based FMC observations of FMC represents an important opportunity to assess the conditions that contribute to severe wildfire behaviour.

Indices such as the Normalized Difference Vegetation Index (NDVI; Tucker 1979), the Normalized Difference Moisture Index (NDMI), and the Visible Atmospherically Resistant Index (VARI; Rao et al. 2020) are sensitive to vegetation water content (Schneider et al. 2008; Gitelson et al. 2002; Rao et al. 2020). Some indices, such as the Normalized Multiband Drought Index (NMDI) and the Green Normalized Difference Vegetation Index (GNDVI), have been used to estimate soil and grassland moisture conditions (Wang and Qu 2007; Bao et al. 2022). Pre- and post-fire imagery is also used for assessing burn severity with metrics like the differenced Normalized Burn Ratio (dNBR; Key and Benson 2006; Kurbanov et al. 2022). Together, these remote sensing tools provide a framework to evaluate how pre-fire FMC relates to wildfire outcomes across forest types in central BC. Multispectral data from the Sentinel-2 constellation, part of the European Space Agency (ESA) Copernicus program (ESA 2023; Drusch et al. 2012), have a high spatial resolution (10–30 m resolution) and a revisit interval of 5 days. These data have been used previously to estimate both fuel moisture (Marino et al. 2020; Costa-Saura et al. 2021) and burn severity (Quintano et al. 2018; Llorens et al. 2021).

Using a combination of ground-based observations and remote sensing imagery from central BC, this study addresses the following research questions:

1. How does FMC vary between old natural forests, juvenile planted stands, and the open conditions found in recent clearcuts?
2. How do ground-based observations of FMC content relate to remote sensing indices?
3. Do pre-fire estimates of FMC derived from remote sensing indices explain the variation in wildfire severity and the existence of some juvenile wildfire skips in central BC?

2 | Study Area

Ground observations of FMC were collected at six research locations unaffected by wildfire near Prince George and Smithers in central BC (Figure 1) in the summers of 2021 and 2022. These sites are broadly classified as being in the Sub-Boreal Spruce (SBS) zone under British Columbia's biogeoclimatic ecosystem classification (BEC) system (Meidinger et al. 1991). The SBS zone is dominated by mature coniferous forests consisting of spruce (*Picea glauca*, *Picea engelmannii*, and their natural hybrids), subalpine fir (*Abies lasiocarpa*), and lodgepole pine (*Pinus contorta*). Other tree species found in this zone include interior Douglas-fir (*Pseudotsuga menziesii var. glauca*) and black spruce (*Picea mariana*) in eastern subzones, with black spruce and tamarack (*Larix laricina*) more abundant on poorly drained terrain, and with trembling aspen (*Populus tremuloides*) and paper birch (*Betula papyrifera*) more abundant in younger stands (Meidinger et al. 1991).

Cool and moist climates characterize the SBS region, with mean annual temperatures between 0°C and 5°C, and mean annual precipitation between 500 mm and 1500 mm (Meidinger et al. 1991). The terrain is characterized by rolling hills, flat plateaus, and gentle slopes, with well-drained soils and scattered wetlands (Demarchi 2011).

Three wildfire case study areas (yellow polygons, Figure 1) were also selected for this research: the 2017 Plateau Complex wildfire, the 2018 Shovel Lake wildfire, and the 2018 Nadina Lake wildfire (red polygons, Figure 1). These areas were selected based on their proximity to the FMC data collection sites, similarities in BEC zone and stand composition (including a balanced portion of juvenile, mature, and open stands), and date of burn (2017 or 2018).

- Juvenile: Lodgepole pine trees have been planted after the primary forest had been logged. Juvenile forests are dense,

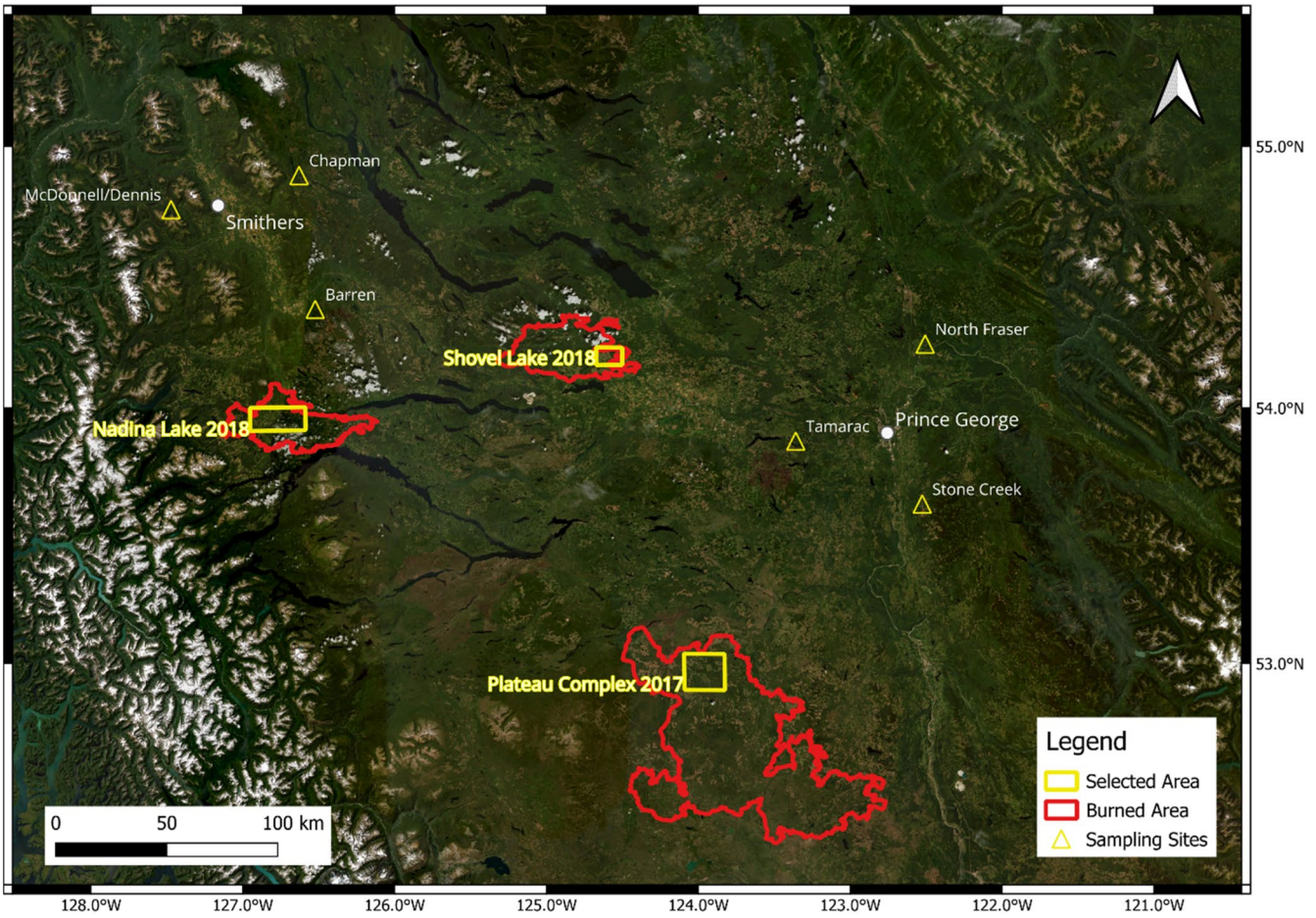


FIGURE 1 | Fuel moisture sample collection sites in 2021/2022 and case study areas (red) from Plateau Complex in 2017, Nadina Lake and Shovel Lake fires in 2018, where yellow polygons indicate areas selected for remote sensing analysis. Background imagery from Esri, Maxar, Earthstar Geographics, and the GIS User Community. "World Imagery" [basemap]. ArcGIS Online. Accessed 2025-09-08. Each field data collection site had three co-located stand types with the following characteristics (Burton 2023).

with only 2–3 m separating each tree; stands are 20–40 years old.

- Open: recently logged, relatively open land with widely spaced, recently established pine seedlings that are 3–7 years old.
- Mature: stands that have never been logged; they are characterized by a variety of trees older than 120 years, with various tree species (lodgepole pine, hybrid white spruce, subalpine fir, and interior Douglas-fir) and lesser amounts of broadleaf species such as black cottonwood (*Populus balsamifera ssp. trichocarpa*) and paper birch, at low densities, and with irregular spatial arrangements.

3 | Methods

3.1 | Field Observations of Fuel Moisture Content

In the summers of 2021 and 2022, samples of foliage (older than one year), fine woody debris, and duff were gathered from the six research sites (Figure 1). Additional microsite information, such as local overstory tree species and sunlight exposure on fuel, was noted during sample collection, as they can impact moisture conditions. Ideally, field sample collection would align with satellite overpasses for a direct comparison between field-observed FMC and remote sensing data. Sentinel 2 collects data at approximately noon local time every 5 days. However, sample collection times typically varied between 10:30 and 15:00 Pacific Standard Time (PST) and did not always match satellite overpass dates due to weather, transportation, schedules, and labour constraints.

In 2021, twelve samples were obtained at the paired juvenile and mature sites near Prince George at each visit: three subsamples each for duff and fine woody debris, as well as three subsamples from higher (4–6 m) and lower (1–2 m) tree foliage. Duff samples were collected from the fermentation and humus layers of the forest floor, below any living moss, typically at depths of 2–5 cm from the surface or 5–10 cm below the top of any dense blankets of feather moss. To assure uniformity, fine woody debris samples were restricted to dead woody material 2–7 mm in diameter, found exposed and loose on the surface of the forest floor. At the Prince George sites, duff and fine woody debris were collected from both sun-exposed and shaded areas, while at the Smithers sites, samples were taken from various spots within each stand to ensure representation and a blend of moisture data from different light conditions. In 2022, lower-level foliage wasn't gathered due to increased sampling frequency and a shortage of sample tins.

At the open sites, nine samples were collected from lower foliage only during each visit, as high foliage does not exist in those areas. Samples were transported in plastic ziplock bags or tightly sealed metal tins to minimize moisture loss and were subsequently weighed and then oven-dried to constant weight in aluminium baking cups or opened metal tins. Moisture content was calculated by drying duff, fine woody debris, and foliage samples in an oven at 100°C for 24 h, a procedure consistent with established FMC measurement protocols and allowed us to process a large volume of samples with the available oven space (Viegas et al. 1992). Top-loading balances were used to measure foliage weights to 0.001 g and duff and fine woody debris to 0.01 g. After drying, the tins were weighed again. Sample mass was calculated by subtracting the weight of the empty tins and lids from both the dry and wet weights.

FMC was then calculated as the percent difference between a sample's fresh weight (M_F) and dry weight (M_D), expressed relative to the sample's dry weight (Equation 1, Chuvieco et al. 2003):

$$\mathrm{FMC} = \left(M_F - M_D\right) / M_D \times 100 \quad (1)$$

Data collected during rainy periods or immediately after rainfall, where water was present on the fuel surface, was excluded. Foliage from tree species other than pine, spruce, fir, or Douglas-fir was also omitted from the analysis. Foliage data from two summers of fieldwork was categorized by species, and their mean, maximum, and minimum values were determined. Foliar moisture content was only compared with remote sensing indices in juvenile and mature stands, while duff moisture content and fine woody debris moisture content were compared with remote sensing indices in open stands.

For each date of observation, the three subsample FMC values for each fuel type (foliage, fine woody debris, and duff) from each stand and date were averaged, then plotted and compared to visualize forest fuel conditions in different stands. Mann–Whitney U tests were conducted in Python (using the *scipy.stats* package) to ascertain if FMC levels varied significantly among different tree species and different stand types throughout the summers of 2021 and 2022. Averaged FMC levels in different stands and sites were subsequently compared with remote sensing indices, as detailed below.

3.2 | Remote Sensing Indices and Fuel Moisture Content

Surface reflectance data from Sentinel-2 satellites were used to calculate time-series of remote sensing indices related to vegetation greenness and moisture over the field sampling areas from 1 May–15 September (2021 and 2022). As Sentinel-2 bands were shifted in 2022 (Google Earth Engine 2022), atmospherically corrected and harmonized surface reflectance data were obtained through Google Earth Engine (GEE, Gorelick et al. 2017) data catalogues for 2021 and 2022 to maintain consistency. A 30 m buffer was applied to the centroid of each GPS-determined sampling location (Figure 2) to represent the spatial range of

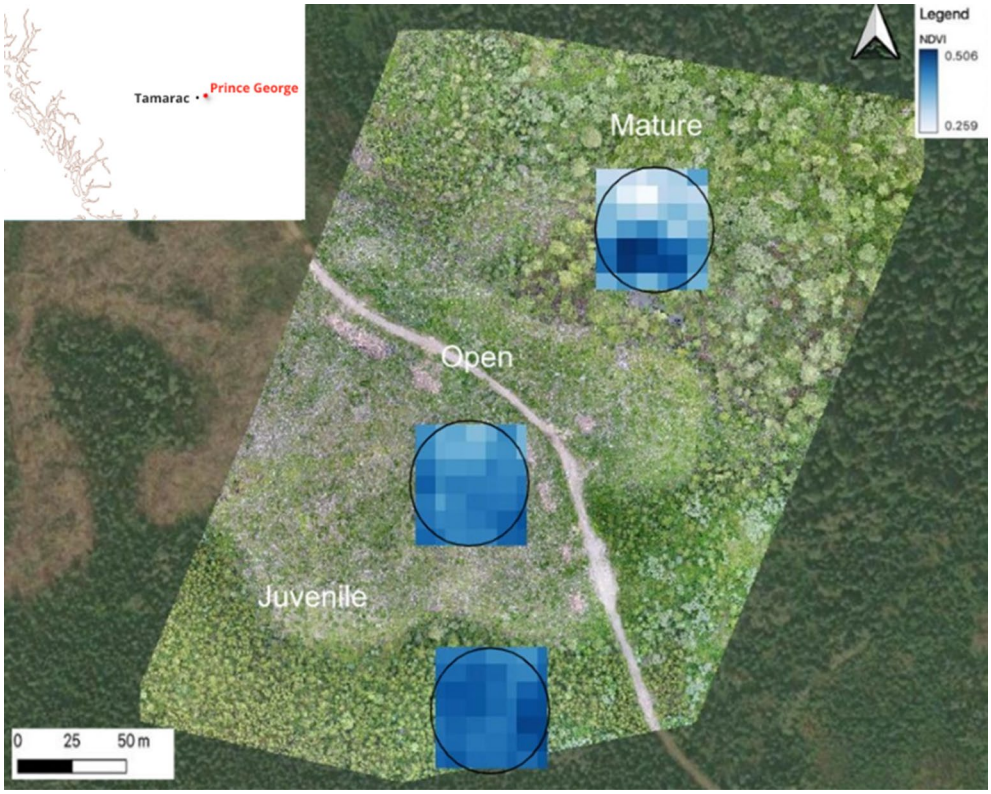


FIGURE 2 | An example of Sentinel-2 Normalized Difference Vegetation Index (NDVI) values (10 m resolution) for three stand types at the Tamarac sample site near Prince George. NDVI was derived on July 20th, 2022, and high resolution RPAS imagery was collected in June 2021. Background imagery from Esri, Maxar, Earthstar Geographics, and the GIS User Community. "World Imagery" [basemap]. ArcGIS Online. Accessed 2025-09-08.

sample collection, and individual bands were clipped to the buffered area. High-resolution Remotely Piloted Aircraft System (RPAS) imagery was collected at three of the sampling sites (e.g., Figure 2) to ensure that the buffered area for Sentinel-2 data collection remained within its respective forest type.

Calculated remote sensing indices are strongly affected by the presence of clouds, cloud shadows, or wildfire smoke. All images were first manually examined for wildfire smoke, and we calculated NDVI thresholds to identify and remove cloud-obscured or cloud-shadowed pixels that fell within the buffer zone of each field sampling point (See Data S1).

Time series of NDVI, NDMI, NMDI, VARI, and GNDVI (see Table 1 for equations and bands used) were calculated from filtered Sentinel-2 data extracted for each stand. Locally Weighted Scatterplot Smoothing (lowess) functions were used to generate continuous values of the remote sensing indices (Cleveland 1979; Moreno et al. 2014) to match the dates of FMC field sampling and avoid issues with mis-matched satellite overpasses and field observations. The smoothing parameter, which controls the balance between the fit to the data and the degree of smoothing applied to the curve, was set at 0.4 (Figure 3).

TABLE 1 | Sentinel 2 band indices used in this study (Data source: USGS, Sentinel Hub).

Remote sensing indices/ Application	Band combinations
NDVI: Measure live green vegetation	(B8 − B4)/(B8 + B4)
NDMI: Measure crop water stress level	(B8 − B11)/(B8 + B11)
NMDI: Measure soil/vegetation moisture	(B8a − (B11 − B12))/ (B8a + (B11 − B12))
VARI: Estimate vegetation fraction	(B3 − B4)/(B3 − B4 − B2)
GNDVI: Measure vegetation greenness	(B8 − B3)/(B8 + B3)
dNBR: Estimate burn severity	Δ(B8 − B12)/(B8 + B12)[a]

[a]Δ refers to the difference between post- and pre-fire imagery.

Using the data from the Prince George and Smithers sites, remote sensing indices extracted from the lowess smoothed time series were compared to foliar moisture content observations at juvenile and mature sites, and to duff and fine woody debris moisture content values at all stands. Ordinary least squares (OLS) linear regression models were calculated using Python's scikit-learn library to relate observed FMC to remote sensing indices, and goodness-of-fit statistics (R^2 and p-values) were computed to evaluate model performance. To account for variability between sites, vegetation indices (e.g., NDVI) were normalized by dividing each value by the mean value for its respective site. This approach standardizes each index relative to its local average, allowing for inter-site comparison of temporal patterns (Jiang et al. 2008). The resulting regression coefficients were then used to estimate FMC from remote sensing indices for the testing data, and an unbiased estimate of the root mean square error (RMSE), mean absolute error (MAE), and mean bias error (MBE) was calculated.

3.3 | Remote Sensing and Fire Severity Case Studies

The third aspect of this research investigates the relationship between wildfire burn severities and pre-fire moisture contents estimated from remote sensing indices in stands of different ages at three recent wildfire complexes (Figure 1, Table 2). Within the perimeter of each wildfire complex, areas that contained a mix of burnt and unburnt forest and a combination of different

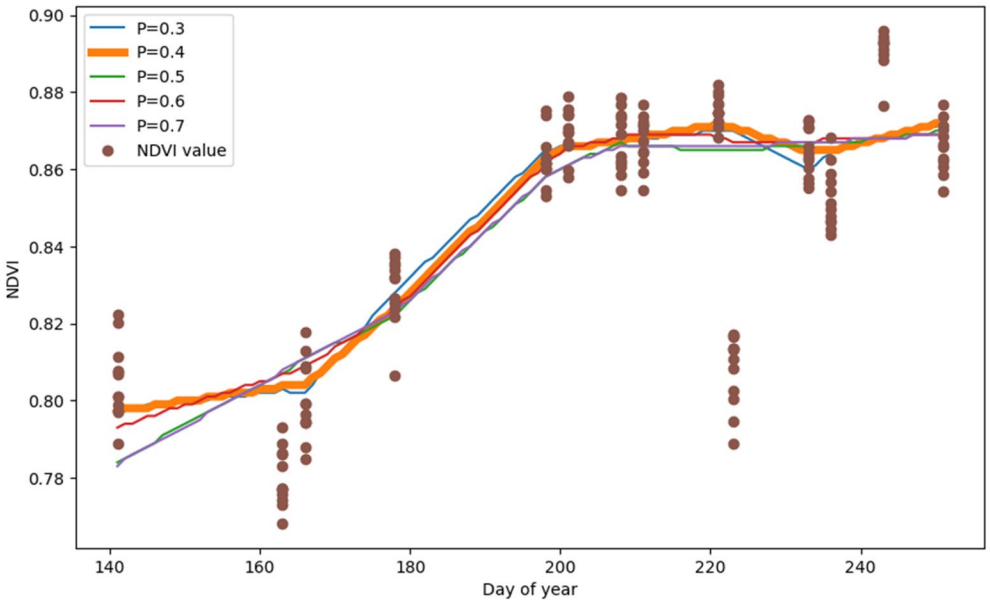


FIGURE 3 | Example of lowess smoothing of NDVI, at Tamarac juvenile site in 2022, with the smoothing parameter (degree of smoothing) set to $p = 0.3$, 0.4, 0.5, 0.6, and 0.7.

TABLE 2 | Wildfire burned case study areas and areas (in hectares) selected for remote sensing analysis, along with the broad stand structure breakdown for each selected area.

Fire ID	Fire Name	Total wildfire area, ha	Selected Area, ha	Juvenile (%)	Mature (%)	Open (%)
C10784	Plateau complex	521 012	78 427	23.49	55.08	21.43
R21721	Nadina Lake	86 766	68 142	32.76	49.38	17.86
R11498	Shovel Lake	79 192	24 435	26.67	40.17	33.16

TABLE 3 | Burn severity levels obtained by calculating dNBR, proposed by USGS (Zhu et al. 2006).

Severity level	dNBR range (scaled by 10^3)
Unburned	−500 to 100
Low severity	+100 to +269
Moderate-low severity	+270 to +439
Moderate-high severity	+440 to +659
High severity	+660 to +1300

forest stand ages were selected (yellow rectangles within red polygons, Figure 1). Characteristics of these regions are given in Table 2.

For this component of our study, we define mature forests as stands older than 60 years, juvenile stands as those logged 10–60 years before 2017–2018, and recently logged areas (open) are those logged since 2007. Vegetation resource inventory (VRI) data (Government of British Columbia 2018) were used to map juvenile and mature forest stands as it provides age information for most forest polygons, including primary forests that have never been logged. A separate database on harvest areas provided by the Government of BC was used to map recently logged forests as it provides more recent and accurate information on logging activity with silviculture updates (Government of British Columbia 2018).

For each of the case study regions, pre-fire Sentinel-2 imagery was obtained as close as possible to the date of wildfire occurrence to calculate remote sensing indices and estimate fuel moisture contents across different stand types. Post-fire imagery was captured on the closest smoke-free and cloud-free day after the wildfire. Both pre- and post-fire images are required to calculate dNBR following the equation in Table 2. While research on wildfire severity using Landsat TM/ETM data provides widely used guidance for converting dNBR values into burn severity categories (Table 3; Zhu et al. 2006), previous research indicates their threshold is similar (Sobrino et al. 2019). We recognize that spectral differences between Landsat and Sentinel-2 sensors mean that these thresholds cannot be directly transferred. In this study, the thresholds are therefore presented only as a general reference to illustrate patterns of post-fire burn severity, rather than as definitive classifications.

As the pre-fire and post-fire imagery used in this analysis is not harmonized (i.e., not compatible with relations developed using harmonized data, Section 3.2), we had to adjust reflectance values for the 2017 imagery. To do so, we performed simple linear regressions between harmonized (Level 2A SR) and non-harmonized (Level 1 C) (TOA) data available in 2021 (Figure S4) and used these regression equations to adjust the 2017 reflectance before calculating pre-fire indices (Hajj et al. 2008).

Generalized relations between remotely sensed data and FMC are required for application over large regions. Since each sample collection site has its own unique forest composition (e.g., canopy density, tree species, and tree ages), topographic characteristics (e.g., slope and aspect), and site-specific factors such as microclimate, soil type, and stand disturbance or management history, directly comparing remote sensing indices across all sites with observed FMC may not be appropriate. To mitigate the influence of site-specific characteristics, we normalized the remote sensing indices by dividing the difference of each index and their minimum value by the difference of their maximum and minimum value for that site (Cao et al. 2017).

$$V'_{i,j} = \frac{V_{i,j} - \min\left(V_j\right)}{\max\left(V_j\right) - \min\left(V_j\right)} \tag{2}$$

where $V'_{i,j}$ ranges from 0 to 1, and is the normalized value of a remote sensing index $\left(V'_{i,j}\right)$ at site j.

Once 2017 remote sensing band values were adjusted to the same scale as 2021 and 2022 harmonized data, the pre-fire indices were normalized according to Equation (2), and significant regressions identified in Section 3.2 were used to estimate pre-fire FMC in the different case study areas and stand types. The statistical significance of the relationship between estimated moisture content and dNBR was evaluated using linear regression in Python (scipy. stats). The p-value was calculated using a two-tailed t-test for the null hypothesis that the regression slope equals zero. Significant relationships were defined as those with $R^2 > 0.1$ and $p < 0.05$. As burn severity can also be assessed as a categorical variable, t-tests were further used to test for differences in estimated moisture content between different stand types and case study areas.

4 | Results

4.1 | Field Observations of Moisture Content

A total of 6116 individual subsamples of foliage, fine woody debris, and duff were collected from open, juvenile, and mature conifer forest stands, with averaged FMC calculated at daily intervals during the summers of 2021 and 2022. Summaries

TABLE 4 | The mean and standard deviation of daily averaged FMC for duff and fine woody debris from different stands in 2021 and 2022.

Type of samples	Duff			Fine woody debris		
Stand type	**Juvenile**	**Mature**	**Open**	**Juvenile**	**Mature**	**Open**
Number of subsamples	709	707	666	676	668	664
Number of samples	132	131	132	132	132	132
Mean MC (%)	142.8[ab]	164.6[a]	129.0[b]	52.4[b]	51.9[b]	32.4[a]
Standard deviation (SD, %)	78.0	84.8	78.9	37.8	39.0	33.4

Note: Superscripts denote results of Mann–Whitney U-tests, where the shared letters in the same category (duff or fine woody debris) indicate no significant difference at the $p = 0.05$ level.

TABLE 5 | The mean and standard deviation (SD) moisture content for foliage from different stands and tree species in 2021 and 2022 (DFir is Douglas-fir).

	Juvenile			Mature				Open		
Foliage type	**Pine**	**Spruce**	**Fir**	**Pine**	**Spruce**	**Fir**	**DFir**	**Pine**	**Spruce**	**Fir**
Subsamples	545	66	56	17	124	485	17	621	6	44
Samples	111	21	23	6	49	108	6	113	3	15
Mean moisture content (%)	112.3	105.6	112.9	105.6	109.8	110.5	143.9	129.2	113.4	116.6
SD (%)	15.1	22.1	33.6	4.8	28.5	21	76.8	27.8	6.83	20.8

Note: No differences among these conifer species were significant within any stand type.

TABLE 6 | The mean and standard deviation (SD) for average daily foliar moisture content, aggregated across all tree species, for different stand types in 2021 and 2022.

	Juvenile stands	Mature stands	Open stands
Number of subsamples	775	757	695
Number of samples	123	123	124
Mean moisture content (%)	112.8[b]	112.2[b]	127.8[a]
SD (%)	15.82	20.14	26.98

Note: Superscripts denote results of Mann–Whitney U-tests, where stand types sharing the same letter are not significantly different at the $p = 0.05$ level.

of the daily average FMC for different observation sites, forest stands (juvenile, mature, and open), as well as different types of fuel (duff and fine woody debris) are presented in Table 4. Information on the total number of daily observation means and standard deviations for each category is also included in Table 4.

4.1.1 | Duff Moisture Content

The average daily moisture content for duff (Table 4) varied among stand types. Statistically significant differences between average duff FMC in mature stands (164.6%) and juvenile stands (142.8%) were identified using the non-parametric Mann–Whitney U test and a significance threshold of 0.05. The average daily duff FMC at open sites (129%) was not significantly lower than that observed at juvenile stands, while it was significantly lower than mature stands.

4.1.2 | Fine Woody Debris Moisture Content

The average daily FMC of fine woody debris in juvenile stands (52.4%) and mature stands (51.9%) was not significantly different (Table 4). However, for open stands, the daily averaged FMC for fine woody debris was 32.4%, which was significantly ($p < 0.05$) lower than that found in both juvenile and mature stands.

4.1.3 | Foliage Moisture Content

Observed moisture contents of live foliage were examined to test for FMC differences among species and stand types (Table 5). Differences in sample size limit the reliability of species comparisons but are shown here to justify the aggregation of samples from different species across stand types.

In juvenile stands, lodgepole pine (Pine, Table 5) foliage had an average moisture content of 112.3%, compared to 112.9% for subalpine fir (Fir, Table 5) and 105.6% for spruce; these differences were not statistically significant. Similarly, there were no significant differences observed among species in the mature stands (105.6, 109.8, 110.5, and 143.9%) for pine, spruce, fir, and Douglas-fir (DFir), respectively (Table 5). Foliage fuel moisture content values in open stands averaged 129.2, 113.4, and 116.6% for pine, spruce, and fir, respectively, again with no significant differences among them.

As we found no statistically significant differences in foliar moisture content among conifer tree species in all stands, foliar moisture contents were aggregated by stand type (Table 6). Aggregated foliar moisture content were similar in mature (112.2%) and juvenile (112.8%) stands and were not significantly different. However,

foliar moisture content in open stands (127.8%) was significantly higher than that found in both juvenile and mature stands.

4.2 | Estimating FMC With Sentinel-2 Data

For each sampling site, remote sensing indices from 1 May to 15 September (2021 and 2022) were extracted with Google Earth Engine (GEE). With Sentinel-2 data, between 55 and 62 images were acquired for each site (Table 7), but due to clouds, cloud shadows, and smoke created by wildfires, the number of images used in this analysis is lower (from 5 to 19 images in 2021 and from 10 to 15 images in 2022).

Time series of the five indices obtained for the Tamarac site, and the lowess smoothers used to extract daily values are shown as an example in Figure 4. Seasonal trends in the indices and differences between stand types can be observed. For example, juvenile stands have the highest value for all indices, followed by mature and open sites.

Average daily FMC measured at each site was regressed against same-day normalized remote sensing indices estimated from the loess smoothed data (examples for foliage moisture content are shown in Figure 5). Regression analyses reveal mostly weak relations between remotely sensed and ground-based data (Table 8). All relationships indicate that higher foliage and duff moisture contents are associated with remote sensing indices for greenness and moisture content, but relationships with fine woody debris moisture content were not significant. A maximum R^2 of 0.31 ($p < 0.05$) was found between normalized NDVI and foliage moisture content in mature stands during 2021 and 2022, while GNDVI and NDMI showed stronger relationships than other indices in most stands. The RMSE for estimated moisture contents ranged between 11.88% and 79.60%, with MAE values spanning 9.22% (NMDI at juvenile foliage) to 62.47%, and MBE values close to zero across all cases (Table 8).

TABLE 7 | Total number of Sentinel-2 scenes and the number of valid scenes (after removal of those with cloud, shadow, and smoke) used for remote sensing analysis in the summer of 2021 and 2022 from each site in the Smithers and Prince George study areas.

Year	Site name	Total scenes	Valid scenes (manual)
2021	Tamarac	55	14
	North Fraser	59	19
	Stone Creek	56	16
	Chapman	55	11
	McDonnell	57	5
	Barren	55	11
2022	Tamarac	57	14
	North Fraser	56	12
	Stone Creek	62	15
	Chapman	56	12
	Dennis	55	10
	Barren	55	13

4.3 | Estimated FMC and Burn Severity

Pre-fire remote sensing indices were used to estimate duff and foliage FMC following the equations in Table 8. Pre-fire remote sensing indices of each case study area were first normalized according to the min/max values (Equation 2), then converted to estimated FMC and compared with dNBR (Figure 6 and Figure 7). Example images of dNBR and estimated FMC at the case study area can be found in Data S1. Notably, for estimated foliage moisture content, Nadina juvenile ($R^2 = 0.29$) and Shovel mature stands ($R^2 = 0.1$) exhibited moderate correlations, all with highly significant p-values ($p < 0.01$), suggesting a meaningful association between burn severity and foliar moisture in these stands. Similarly, estimated duff moisture content at Nadina and Shovel open stands has 0.17–0.29 R^2, with p-values < 0.01. In contrast, the remaining stands showed weak ($R^2 < 0.1$) relationships, indicating that dNBR may not be a reliable predictor of FMC in those conditions. What's more, even for the locations that have significant relationships, some overall trends are unclear, such as in the Nadina Lake fire where high estimated FMC indicated high dNBR in open stands, while the trend in the Shovel Lake fire is the opposite.

Comparisons of estimated FMC between unburned and moderate-to-high burn severity conditions revealed significant differences across all sites and stand types for both duff and foliage layers ($p < 0.01$ in all cases; Table 9). For duff, mature stands consistently exhibited the highest estimated moisture contents. Counterintuitively, some unburned stands had lower levels of estimated duff moisture content than moderate-to-high burn severity stands, particularly in the Nadina (175%–200%) and Shovel (192%–202%) case study areas. Conversely, unburned open stands showed higher duff moisture content estimates at Nadina (131%–161%) and Plateau (130%–132%), while at Shovel, moderate-to-high severity regions exhibited higher pre-fire duff moisture content estimates than unburned areas (147% vs. 129%). Juvenile stands displayed minimal or variable differences in estimated duff moisture content between burn severity classes.

In mature stands, moderate-to-high severity regions showed lower pre-fire foliar moisture content estimates at Nadina (98%–110%) and modest reductions at Plateau. In contrast, mature stands at Shovel exhibited slightly higher foliar moisture content estimates (104%–108%). Juvenile stands again showed minimal differences across sites. Although these differences were statistically significant, some were small or counterintuitive, indicating that pre-fire moisture content may not be the primary driver of burn severity in these case studies.

Mixed-effects modelling with wildfire location as a random factor further confirmed these patterns. Mature stands had significantly higher estimated duff moisture content than juvenile stands (coef = 45.89, $p < 0.001$), while differences in foliar moisture content estimates were positive but modest (coef = 1.75, $p < 0.001$). These results confirm that stand type has a statistically significant effect on pre-fire moisture content estimates, particularly for the duff layer, whereas differences in estimated

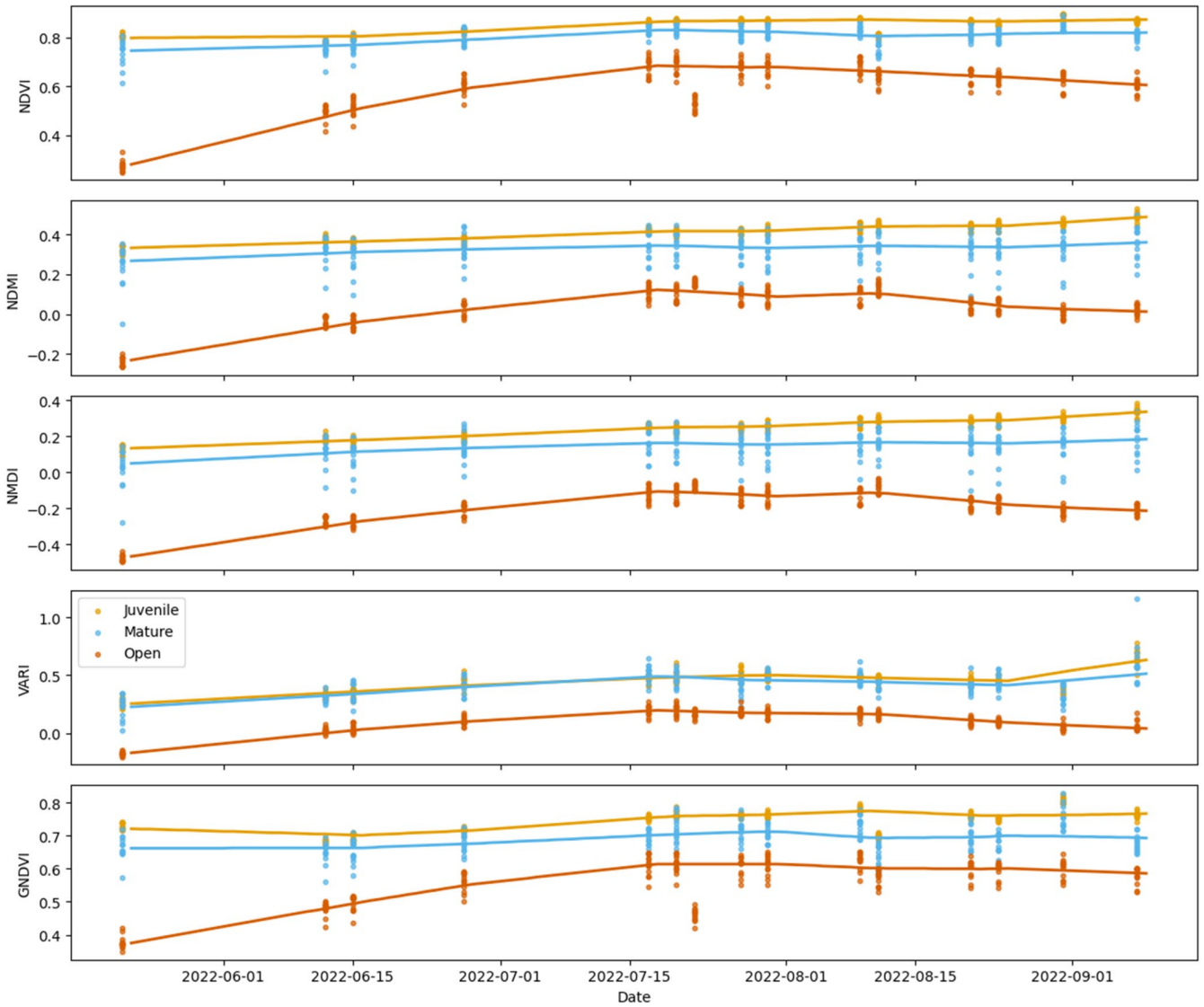


FIGURE 4 | Remote sensing indices derived from Sentinel-2 data at the Tamarac site for different stand types, 2022. Solid lines are the lowess smoothers (span = 0.4) and each point represents a pixel index value when Sentinel-2 passed. Yellow points and lines represent values for juvenile plantations, blue denotes mature primary forest, and orange denotes recently planted open cutblocks.

foliar moisture content are smaller and less pronounced, consistent with field observations.

5 | Discussion

Ground-based sampling identified significant differences in moisture content among different stand types (open, mature, juvenile) and fuels (duff, fine woody material, and foliage). As no significant difference in foliar moisture content was observed among the conifer species sampled, we were able to pool those measurements for use in evaluating satellite-based estimates of moisture content. Several remote-sensing indices showed weak but significant relationships to ground-based measurements of fuel moisture, with GNDVI being most promising, although NDMI and NDVI were more closely associated with foliage or duff moisture content in specific stand types. When applied to fuel conditions found prior to three large wildfires in central British Columbia, those relationships predicted foliage moisture content that was 6%–58% higher in forest stands that later remained unburned than nearby burned forest. We here discuss how these findings relate to comparable studies reported in the literature, and how they might be refined for improved use in wildfire preparedness and management.

5.1 | Field Observations

In 2021 and 2022, we find that duff had a significantly higher daily averaged FMC in mature stands than that found in juvenile and open stands. For fine woody debris, the daily averaged FMC was similar in mature and juvenile stands, with no significant difference. However, open stands had a significantly lower daily average duff and fine woody debris moisture content than juvenile and mature stands, as expected from their greater exposure to the drying effects of sunlight and wind. In contrast, recent clearcuts (which we characterized as open sites) had a significantly higher daily average foliage moisture content in the actively growing young pine trees, while mature and juvenile forests had similar daily average foliage moisture content without significant differences.

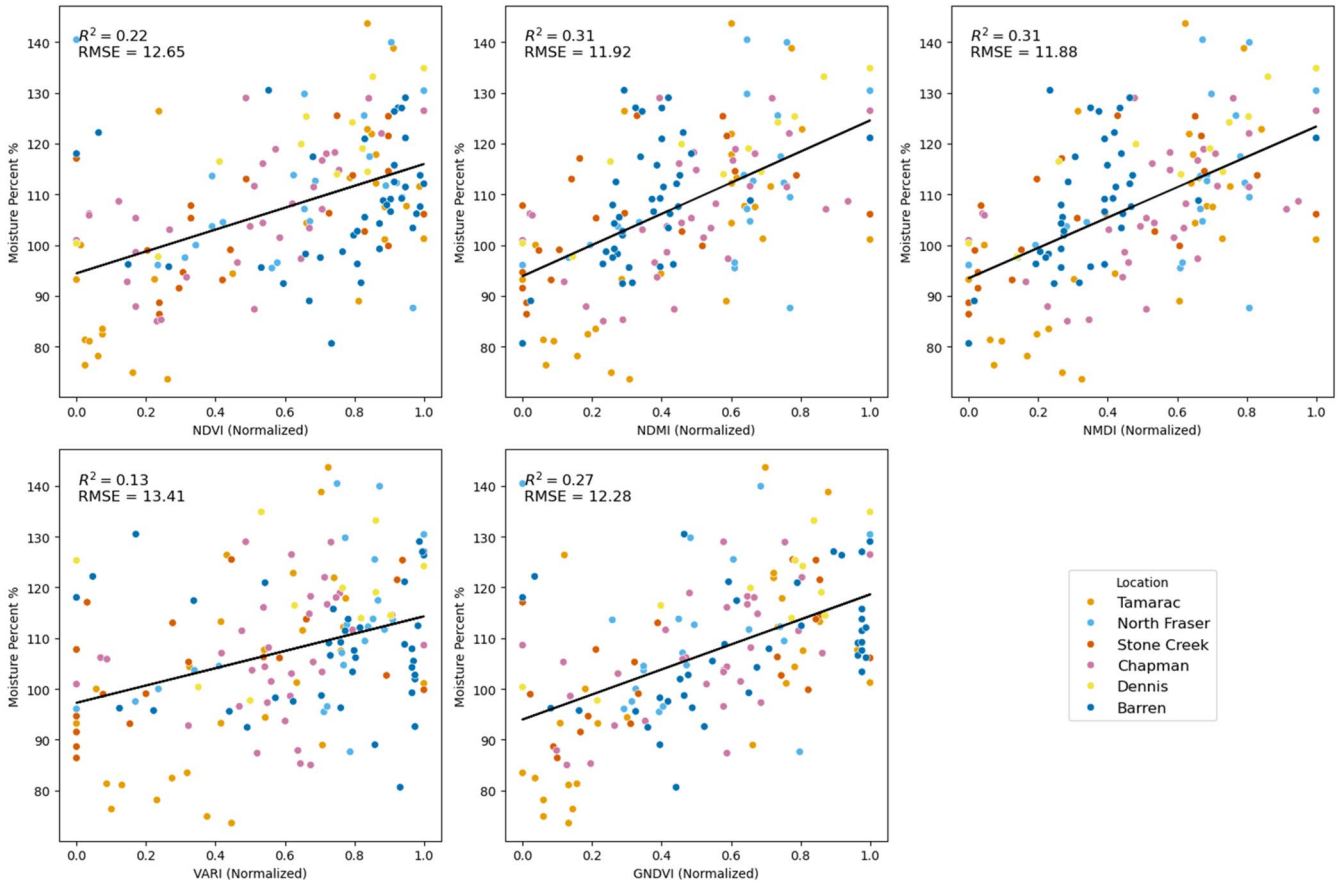


FIGURE 5 | Linear regressions between observed foliage moisture content and normalized same-day remote sensing indices estimated from lowess smoothing at juvenile stands.

TABLE 8 | Significant ($p < 0.005$) linear regressions between FMC and normalized remote sensing indices at different stands, with their R^2 and RMSE values.

Stand type	Fuel type	Indices	R^2	RMSE (%)	MAE	Equation
Juvenile	Foliage	NMDI	0.31	11.88	9.22	FMC = 29.88 * NMDI' + 93.48
Juvenile	Duff	GNDVI	0.11	71.57	57.52	FMC = −50.4 * GNDVI' + 163.96
Mature	Foliage	NDVI	0.31	12.98	10.04	FMC = 30.68 * NDVI' + 88.61
Mature	Duff	NMDI	0.14	79.60	62.47	FMC = −108.22 * NMDI + 218.57
Open	Duff	GNDVI	0.24	67.99	55.13	FMC = −126.26 * GNDVI' + 206.124

Mature forests have deep canopies and a long developmental history over which they shed needles, creating a thicker layer of litter that can trap moisture and slow evaporation, resulting in higher FMC in the duff layer (Harmon et al. 1986). Fine woody debris in mature conifer forests may have undergone more decomposition than in juvenile conifer forests, resulting in a higher overall moisture content; however, this can be offset by the accumulation of new fine woody debris in mature forests (Brown 2003; Harmon et al. 1986). Open stands likely have lower duff and fine woody debris moisture content because of high evaporation rates in the absence of canopy cover. Mature and juvenile forests have denser canopy cover that shades the forest floor and reduces the rate of evaporation, helping to maintain moisture levels in the fine woody debris and duff layer (Wotton et al. 2005). At open sites, conifer foliage was collected from actively growing trees younger than 10 years old. Active growth in younger trees is associated with high overall tissue FMC, and young conifer needles are known to have high FMC (Hatcher 1990; Agee et al. 2002; Lindenmayer et al. 2012).

Although field observations of FMC yield direct estimates of moisture levels in forest fuels, they are time-consuming and costly (Caccamo et al. 2011). Remote sensing indices, as demonstrated in this work, can provide estimates of normalized duff and foliage moisture contents (Figure 5). While there are likely site-specific controls on absolute fuel moisture contents (climate, slope, aspect, soil type, etc.), the normalization across sites can provide relative indications of higher or lower fuel moisture contents.

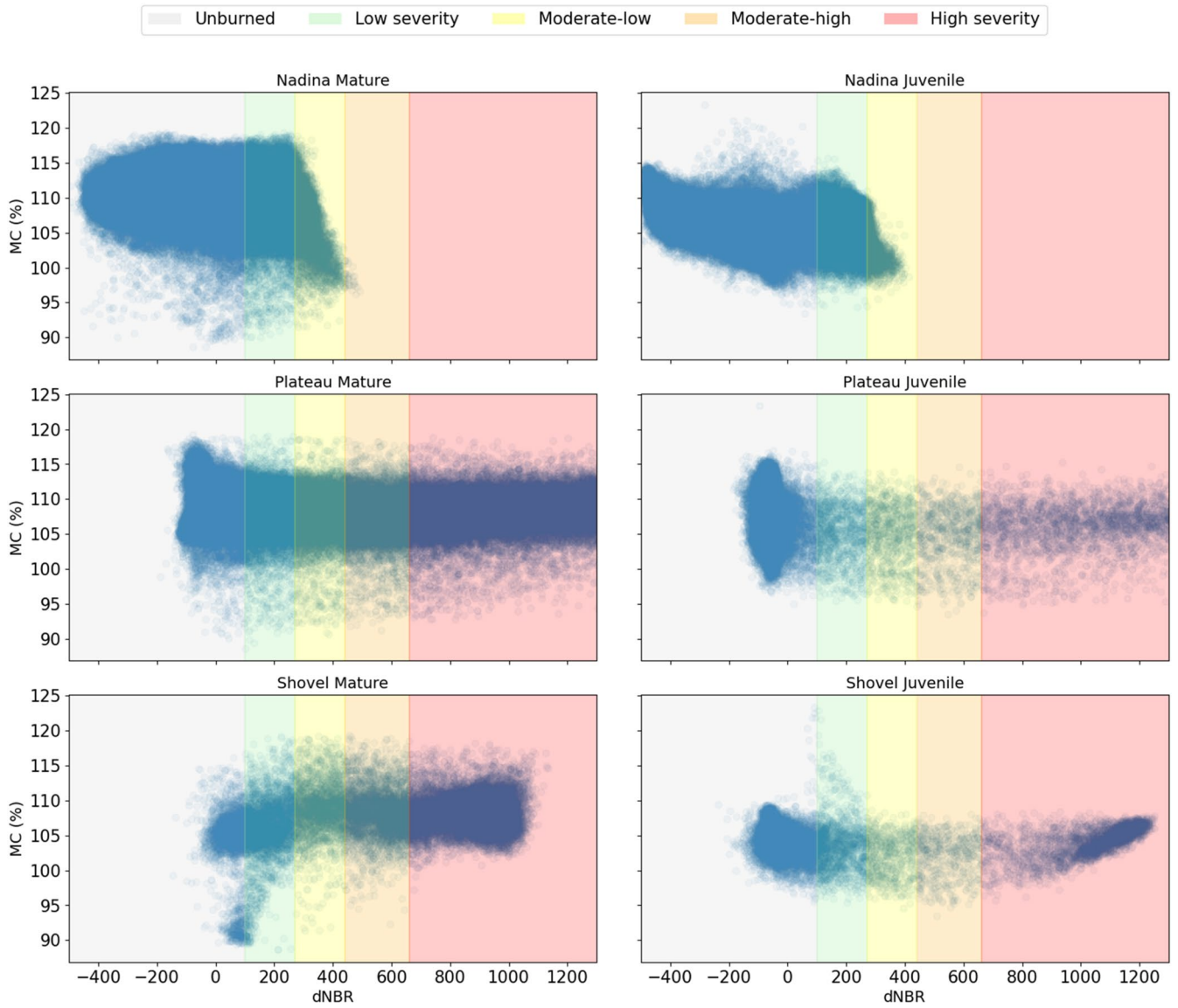


FIGURE 6 | Patterns of estimated pre-fire foliage moisture content for three wildfire case studies, derived using the linear regressions from Table 8. Burn severity classes (Table 3) are shown by the shaded regions; note the fire severity classes are based on Landsat dNBR values and are shown here for illustrative purposes only.

5.2 | Remote Sensing Estimates of FMC

In Section 4.3, remote sensing indices showed significant ($p < 0.001$) relationships with observed fuel moisture content, with R^2 values ranging from 0.10 to 0.31. These moderate relationships are consistent with previous studies showing the challenges of predicting fuel moisture from spectral indices alone (Yebra et al. 2008; Caccamo et al. 2011). The accuracy of this approach depends strongly on the frequency and quality of data collected. For example, during the wildfires in central BC in the summer of 2021, clouds and smoke substantially reduced the number of usable image capture days, leading to gaps in the time series and increasing the potential for inaccuracies in index values derived from smoothing functions (Roy and Joshi 2002; Hilker et al. 2009).

Although matching field sample collection days with satellite overpasses can reduce some of the errors introduced by temporal smoothing, labor constraints prevented the collection of moisture content samples on every clear-sky date. As a result, the use of a lowess smoothing function was still necessary for the 2022 dataset. While this approach helps fill temporal gaps, it can introduce additional errors by failing to capture true index values on certain sampling dates (Hilker et al. 2009). Without more frequent field observations and higher image availability, it remains difficult to accurately align remote sensing and ground-based measures of fuel moisture.

The relationship between fuel moisture content and remote sensing indices is also influenced by ecological and structural factors such as tree species, canopy exposure, and foliage height (Riano et al. 2005). In this study, only three foliage samples were collected per stand per visit, and foliage type and exposure were not consistently controlled. Although daily average foliage moisture content did not differ significantly across species, restricting measurements to a single species and canopy position may yield more representative relationships. Ideally, foliage samples would be collected from tree tops, which are more visible to satellites than the mid- and lower-canopy branches sampled here.

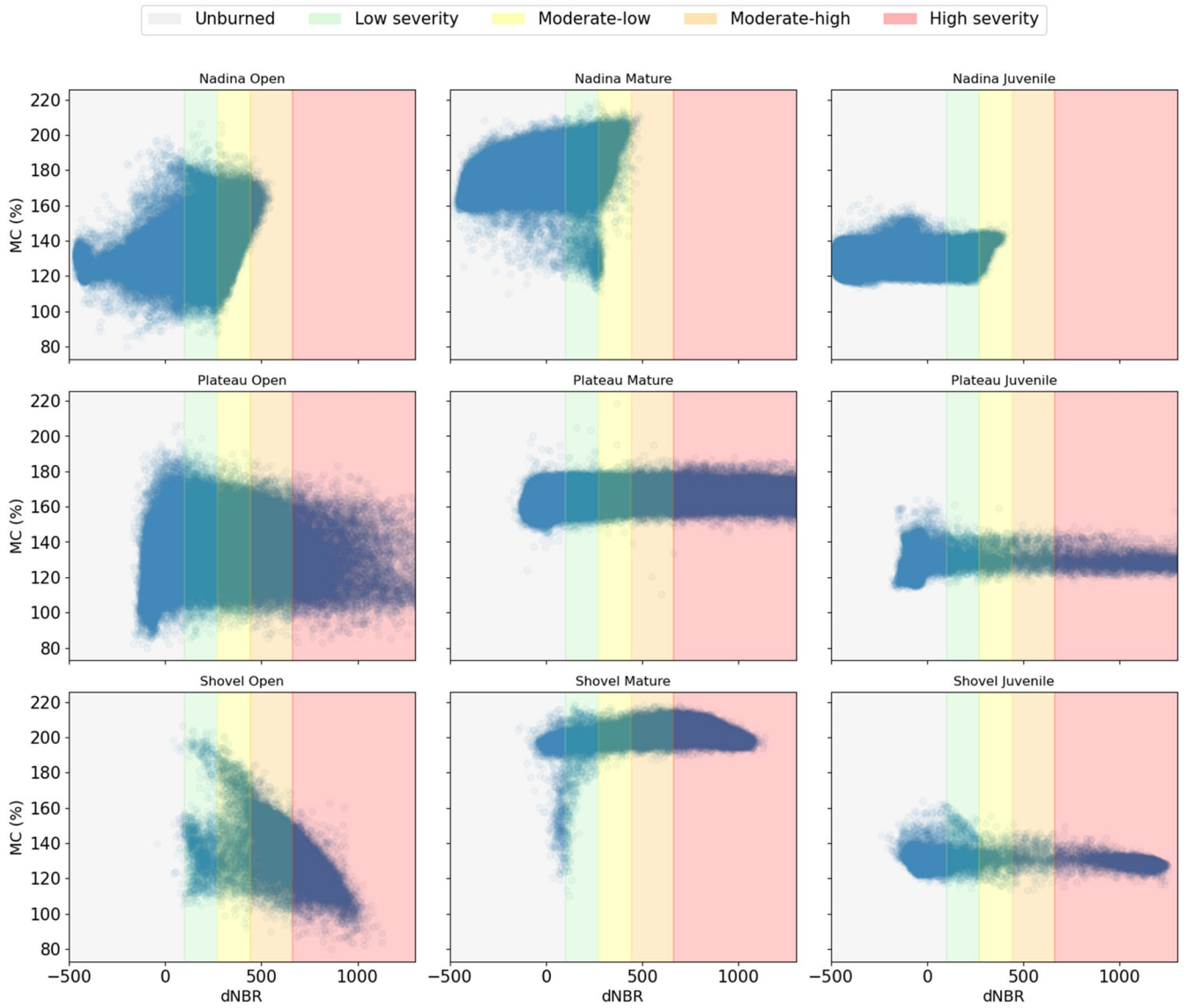


FIGURE 7 | Patterns of estimated pre-fire duff moisture content for three wildfire case studies, derived using the linear regressions from Table 8, burn severity classes from Table 3; note the fire severity classes are based on Landsat dNBR values and are shown here for illustrative purposes only.

TABLE 9 | Mixed-effects model results for estimated pre-fire foliar and duff moisture content: Stand type effects with wildfire location as a random factor.

Variable	Coefficient	Standard error	z-value	*p*-value
Foliar moisture content	1.75	0.009	192.175	<0.001
Duff moisture content	45.89	0.023	2020.811	<0.001

Another limitation arises from the spatial resolution of Sentinel-2 data (10 m), where individual pixels include non-foliage elements such as trails, tree boles, branches, fallen logs, and bare ground (Riano et al. 2005). These mixed-pixel effects can further weaken the correspondence between spectral indices and measured moisture. The frequency and timing of satellite acquisitions may also contribute additional uncertainty. To improve accuracy, future studies could incorporate drone-based multispectral data, which provide much finer resolution and greater flexibility in acquisition timing, or Synthetic Aperture Radar (SAR), which is less affected by clouds and has shown strong potential for monitoring fuel moisture (Yebra et al. 2013; Rao et al. 2020). Collecting imagery closer to the field sampling window would also reduce potential errors associated with rapid changes in weather and moisture conditions.

5.3 | Burn Severity versus Estimated FMC

While forest harvest data from the Government of BC provides mapped areas of recently logged stands, and VRI data included stand age for the three case study areas, there were still some forest polygons with no defined age class. Such limitations could be avoided by restricting remote sensing analysis to only the precise stand types and ages used for ground-based calibration

data. Extrapolating data and relationships from a few ground plots over large areas is always tenuous, due to unavoidable differences in forest type, topography, and climate. Clouds, shadows, and smoke can also decrease the chance of getting pre-fire imagery prior to the wildfire event, which may lead to less accurate pre-fire forest conditions. Variation in the trends observed between estimated FMC and dNBR (e.g., for Shovel Lake open and juvenile stands, Figures 6 and 7) suggests there may be two sub-populations or additional considerations such as unique wildfire behaviour that prevent a single relationship from emerging. This warrants further investigation.

Although our results indicate that there are various relationships between estimated foliage and duff moisture content and burn severity ratios (e.g., in the Nadina and Shovel selected area), we cannot infer that FMC is a decisive factor for forest resistance to wildfire. At the end of summer in 2021, ground-based burn severity assessments were conducted at selected sites in the Plateau Complex wildfire (data not presented). To compare burn severity assessments between remotely sensed and on-site observations, 15 unburned juvenile forest stands (fire skips) and 17 nearby burned stands were visited. When visiting unburned fire skips, it was common to notice that their edges had a relatively higher burn severity than the center of the juvenile forest stand. From burn severity assessments and fieldwork observations, wildfires do not just suddenly stop when they encounter the juvenile stands; rather, they burned the edges of the stands and then spread slowly in the understory and stopped as they reached deeper into the forest. Evidence of low-intensity fire close to the ground, such as scorched tree bases, less surviving moss, and recently established fireweed (*Epilobium angustifolium*), was found frequently within the fire skips (i.e., where the tree canopy did not burn), even far from the edge of the forest. Satellite-based mapping of "unburned" forest may detect unburned overstories, not simply an absence of fire. Open stands and very young juvenile stands elsewhere, on the other hand, are reported to have a higher burn severity potential due to their high levels of woody debris frequently left after previous logging (Brown 2003; Lindenmayer et al. 2009).

Other research in our study area has confirmed that juvenile pine plantations 20–40 years old experience reduced burn severity, and that variation in burn severity is related to differences in stand structure and management practices (Clason et al. n.d.). The high stem density in juvenile pine plantations may play a role in reducing the spread of fire by decreasing wind speed. The models in Section 4.2 reinforce that pre-fire moisture content varies by stand type across all wildfire locations, but the magnitude and ecological relevance of these differences are layer dependent. Additional work (Xiao 2023) documented wind speeds significantly lower in juvenile plantations than in mature and open stands, which may prevent fire spread and the development of crown fires. This highlights the complex interplay between various factors that can influence the impact of wildfires on forests, and the importance of considering a range of factors when evaluating the resistance of forests to fire.

6 | Conclusions

This research compares duff, fine woody debris, and foliage moisture content values measured in mature, juvenile, and open stands near Prince George and Smithers, British Columbia. Burn severities and their relationship to pre-fire remote sensing indices were also analyzed in different stands in three recent wildfires to evaluate the role of estimated fuel moisture contents on burn severity in different stand types.

After comparing observed FMC and normalized remote sensing indices at the different stands and sites, a few relationships can be highlighted. When estimating foliage moisture content in juvenile and mature stands, NDMI and NDVI had higher R^2 values (0.31) and lower *p*-values (less than 0.005) than other indices. When estimating duff moisture content, GNDVI had higher R^2 (0.24 and 0.11) and lower *p*-value (less than 0.005) for open and juvenile stands, and NMDI for mature stands (0.14, <0.005). No significant relationship was found in estimating fine woody debris moisture content in all stands and foliage for open stands. In general, the relationships between remote sensing indices and foliage and duff moisture content were highly significant (extremely small *p* values) but highly variable ($R^2<0.3$). With the impact of satellite visit frequency, band resolution, weather, and the quality and quantity of observational data, it is unlikely that strong and accurate relationships between remote sensing indices and FMC can be obtained.

Three case study areas in central British Columbia were used to examine pre-and post-fire forest conditions through remote sensing. In juvenile stands, our NDMI-based estimates of pre-fire duff moisture content in unburnt areas were higher than in severely burned areas, while no significant trend was found in the association of burn severity and estimated pre-fire foliar moisture content. Thus, while FMC differences in duff and foliage over the course of stand development may be a contributing factor on some sites or under some fire weather conditions, they are clearly not the driving factor in explaining why juvenile plantations can sometimes be skipped by crown fires.

Acknowledgements

This research was supported by a National Science and Engineering Research Council of Canada Discovery Grant to J.M.S. (RGPIN-2019-07112), and a Natural Resources Canada Emergency Management Strategy Program Grant FIREPFC-06 to P.J.B. The BC Wildfire Service assisted in covering field expenses. We thank Morgan Endacott, Clayton Rose, Alexandra Golt, Mackenzie McLean, Dongxu Piao, Shiyuan Jing, and Trevor Schibli for their diligent assistance with recurrent fuel moisture sample collection and weighing. We are grateful to two reviewers and the editor for their comments and suggestions, which have helped improve the manuscript.

Data Availability Statement

Fuel moisture content observations were made available in a publicly available repository (https://doi.org/10.5281/zenodo.17173324). Sentinel-2 remote sensing data can be obtained through Google Earth Engine or Copernicus.

References

Agee, J. K., C. S. Wright, N. Williamson, and M. H. Huff. 2002. "Foliar Moisture Content of Pacific Northwest Vegetation and Its Relation to Wildland Fire Behavior." *Forest Ecology and Management* 167, no. 1–3: 57–66.

Bao, W., F. Yu, Y. Chang, M. Guo, F. Zhou, and C. Zhong. 2022. "Estimation of Fuel Load Using Remote Sensing Data in Hulunbuir Grassland." *Natural Hazards Research* 2, no. 4: 375–383.

Brown, J. K. 2003. *Coarse Woody Debris: Managing Benefits and Fire Hazard in the Recovering Forest. General Technical Report RMS-GTR-105*, 16. USDA Forest Service.

Burton, P., C. Mahood, A. Boxwell, S. Taylor, L. McCulloch, and M. Dale. 2019. "Why Have Recent Mega-Fires in British Columbia Left Some Established Plantations Unburned." In *North American Forest Ecology Workshop, 24 June 2019*. Arizona.

Burton, P. J. 2023. "Understanding the Effects of Forest Management and Prior Disturbances on Forest Fire Risk and Behavior." In *FIREPFC-06 Final Report to Natural Resources*, 38.

Caccamo, G., L. A. Chisholm, R. A. Bradstock, and M. L. Puotinen. 2011. "Assessing the Sensitivity of MODIS to Monitor Drought in High Biomass Ecosystems." *Remote Sensing of Environment* 115, no. 10: 2626–2639.

Cao, F., Z. Yang, J. Ren, M. Jiang, and W. K. Ling. 2017. "Does Normalization Methods Play a Role for Hyperspectral Image Classification?. arXiv preprint arXiv:1710.02939."

Ceccato, P., S. Flasse, and J. M. Gregoire. 2002. "Designing a Spectral Index to Estimate Vegetation Water Content From Remote Sensing Data: Part 2. Validation and Applications." *Remote Sensing of Environment* 82, no. 2–3: 198–207.

Chuvieco, E., I. Aguado, D. Cocero, and D. Riano. 2003. "Design of an Empirical Index to Estimate Fuel Moisture Content From NOAA-AVHRR Images in Forest Fire Danger Studies." *International Journal of Remote Sensing* 24, no. 8: 1621–1637.

Chuvieco, E., I. González, F. Verdú, I. Aguado, and M. Yebra. 2009. "Prediction of Fire Occurrence From Live Fuel Moisture Content Measurements in a Mediterranean Ecosystem." *International Journal of Wildland Fire* 18, no. 4: 430–441.

Clason, A. J., K. M. Hoffman, I. Farnell, S. Coggins, and P. J. Burton. n.d. "Stand Age and Forest Structure Influenced Burn Severity in Sub-Boreal Conifer Plantations. In revision for *Ecosphere*."

Cleveland, W. S. 1979. "Robust Locally Weighted Regression and Smoothing Scatterplots." *Journal of the American Statistical Association* 74, no. 368: 829–836.

Costa-Saura, J. M., Á. Balaguer-Beser, L. A. Ruiz, J. E. Pardo-Pascual, and J. L. Soriano-Sancho. 2021. "Empirical Models for Spatio-Temporal Live Fuel Moisture Content Estimation in Mixed Mediterranean Vegetation Areas Using Sentinel-2 Indices and Meteorological Data." *Remote Sensing* 13, no. 18: 3726. https://doi.org/10.3390/rs13183726.

Danson, F. M., and P. Bowyer. 2004. "Estimating Live Fuel Moisture Content From Remotely Sensed Reflectance." *Remote Sensing of Environment* 92, no. 3: 309–321.

Demarchi, D. A. 2011. "An Introduction to the Ecoregions of British Columbia." In *Ecosystem Information Section*, 163. Ministry of Environment, Government of British Columbia.

Dennison, P. E., M. A. Moritz, and R. S. Taylor. 2008. "Evaluating Predictive Models of Critical Live Fuel Moisture in the Santa Monica Mountains, California." *International Journal of Wildland Fire* 17, no. 1: 18–27.

Drusch, M., U. Del Bello, S. Carlier, et al. 2012. "Sentinel-2: ESA'S Optical High-Resolution Mission for GMES Operational Services." *Remote Sensing of Environment* 120: 25–36.

European Space Agency (ESA). 2023. "Sentinel-2 Annual Performance Report – Year 2022 (Ref. OMPC.CS.APR.001+ – i1r0). Copernicus." https://sentinels.copernicus.eu/documents/247904/4893455/OMPC.CS.APR.001+-+i1r0+-+S2+MSI+Annual+Performance+Report+2022.pdf.

Flannigan, M. D., B. J. Stocks, and B. M. Wotton. 2000. "Climate Change and Forest Fires." *Science of the Total Environment* 262, no. 3: 221–229.

Gitelson, A. A., Y. J. Kaufman, R. Stark, and D. Rundquist. 2002. "Novel Algorithms for Remote Estimation of Vegetation Fraction." *Remote Sensing of Environment* 80, no. 1: 76–87.

Google Earth Engine. 2022. "Harmonized Sentinel-2 MSI: Multi Spectral Instrument, Level-2A (SR) [Earth Engine Dataset]." *Earth Engine Data Catalog*. https://developers.google.com/earth-engine/datasets/catalog/COPERNICUS_S2_SR_HARMONIZED.

Gorelick, N., M. Hancher, M. Dixon, S. Ilyushchenko, D. Thau, and R. Moore. 2017. "Google Earth Engine: Planetary-Scale Geospatial Analysis for Everyone." *Remote Sensing of Environment* 202: 18–27.

Government of BC. 2018. "2018 Annual Forest Inventory Release." Accessed 2024. https://www2.gov.bc.ca/gov/content/industry/forestry/managing-our-forest-resources/forest-inventory/data-management-and-access.

Hajj, M. E., A. Bégué, B. Lafrance, O. Hagolle, G. Dedieu, and M. Rumeau. 2008. "Relative Radiometric Normalization and Atmospheric Correction of a SPOT 5 Time Series." *Sensors* 8, no. 4: 2774–2791.

Harmon, M. E., J. F. Franklin, F. J. Swanson, et al. 1986. "Ecology of Coarse Woody Debris in Temperate Ecosystems." In *Advances in Ecological Research*, edited by A. MacFadyen and E. D. Ford, vol. 15, 133–302. Academic Press.

Hartford, R. A., and W. H. Frandsen. 1992. "When It's Hot, It's Hot... or Maybe It's Not! (Surface Flaming May Not Portend Extensive Soil Heating)." *International Journal of Wildland Fire* 2, no. 3: 139–144.

Hatcher, P. E. 1990. "Seasonal and Age-Related Variation in the Needle Quality of Five Conifer Species." *Oecologia* 85: 200–212.

Hilker, T., M. A. Wulder, N. C. Coops, et al. 2009. "Generation of Dense Time Series Synthetic Landsat Data Through Data Blending With MODIS Using a Spatial and Temporal Adaptive Reflectance Fusion Model." *Remote Sensing of Environment* 113, no. 9: 1988–1999. https://doi.org/10.1016/j.rse.2009.05.011.

Jiang, Z., A. R. Huete, K. Didan, and T. Miura. 2008. "Development of a Two-Band Enhanced Vegetation Index Without a Blue Band." *Remote Sensing of Environment* 112, no. 10: 3833–3845.

Key, C. H., and N. C. Benson. 2006. "Landscape Assessment (LA) Sampling and Analysis Methods." In *FIREMON: Fire Effects Monitoring and Inventory System, General Technical Report RMRS-GTR-164-CD*, edited by D. C. Lutes, R. E. Keane, J. F. Caratti, et al., LA-1-55. USDA Forest Service.

Krawchuk, M. A., S. L. Haire, J. Coop, et al. 2016. "Topographic and Fire Weather Controls of Fire Refugia in Forested Ecosystems of Northwestern North America." *Ecosphere* 7, no. 12: e01632.

Krawchuk, M. A., M. A. Moritz, M. A. Parisien, J. Van Dorn, and K. Hayhoe. 2009. "Global Pyrogeography: The Current and Future Distribution of Wildfire." *PLoS One* 4, no. 4: e5102.

Kurbanov, E., O. Vorobev, S. Lezhnin, et al. 2022. "Remote Sensing of Forest Burnt Area, Burn Severity, and Post-Fire Recovery: A Review." *Remote Sensing* 14, no. 19: 4714.

Lindenmayer, D. B., W. Blanchard, L. McBurney, et al. 2012. "Interacting Factors Driving a Major Loss of Large Trees With Cavities in a Forest Ecosystem." *PLoS One* 7: e000000.

Lindenmayer, D. B., M. L. Hunter, P. J. Burton, and P. Gibbons. 2009. "Effects of Logging on Fire Regimes in Moist Forests." *Conservation Letters* 2, no. 6: 271–277.

Llorens, R., J. A. Sobrino, C. Fernández, J. M. Fernández-Alonso, and J. A. Vega. 2021. "A Methodology to Estimate Forest Fires Burned Areas and Burn Severity Degrees Using Sentinel-2 Data. Application to the October 2017 Fires in the Iberian Peninsula." *International Journal of*

Applied Earth Observation and Geoinformation 95: 102243. https://doi.org/10.1016/j.jag.2020.102243.

Marino, E., M. Yebra, M. Guillén-Climent, et al. 2020. "Investigating Live Fuel Moisture Content Estimation in Fire-Prone Shrubland From Remote Sensing Using Empirical Modelling and RTM Simulations." *Remote Sensing* 12, no. 14: 2251. https://doi.org/10.3390/rs12142251.

McGee, T., B. McFarlane, and C. Tymstra. 2015. "Wildfire: A Canadian Perspective." In *Wildfire Hazards, Risks and Disasters*, 35–58. Elsevier.

Meidinger, D., J. Pojar, and W. L. Harper. 1991. "Sub-Boreal Spruce Zone." In *Ecosystems of British Columbia. Special Report Series 6*, edited by D. Meidinger and J. Pojar, 209–221. British Columbia Ministry of Forests.

Moreno, Á., F. J. García-Haro, B. Martínez, and M. A. Gilabert. 2014. "Noise Reduction and Gap Filling of fAPAR Time Series Using an Adapted Local Regression Filter." *Remote Sensing* 6, no. 9: 8238–8260.

Nolan, R. H., M. M. Boer, V. Resco de Dios, G. Caccamo, and R. A. Bradstock. 2016. "Large-Scale, Dynamic Transformations in Fuel Moisture Drive Wildfire Activity Across Southeastern Australia." *Geophysical Research Letters* 43, no. 9: 4229–4238. https://doi.org/10.1002/2016gl068614.

Norum, R. A., and M. Miller. 1984. "Measuring Fuel Moisture Content in Alaska: Standard Methods and Procedures. Gen. Tech. Rep. PNW-GTR-171. 1984. U.S. Department of Agriculture, Forest Service, Pacific Northwest Forest and Range Experiment Station."

Parisien, M. A., Q. E. Barber, M. L. Bourbonnais, et al. 2023. "Abrupt, Climate-Induced Increase in Wildfires in British Columbia Since the Mid-2000s." *Communications Earth & Environment* 4, no. 1: 309.

Parks, S. A., G. K. Dillon, and C. Miller. 2014. "A New Metric for Quantifying Burn Severity: The Relativized Burn Ratio." *Remote Sensing* 6, no. 3: 1827–1844.

Qi, Y., P. E. Dennison, W. M. Jolly, R. C. Kropp, and S. C. Brewer. 2014. "Spectroscopic Analysis of Seasonal Changes in Live Fuel Moisture Content and Leaf Dry Mass." *Remote Sensing of Environment* 150: 198–206.

Quintano, C., A. Fernández-Manso, and O. Fernández-Manso. 2018. "Combination of Landsat and Sentinel-2 MSI Data for Initial Assessment of Burn Severity." *International Journal of Applied Earth Observation and Geoinformation* 64: 221–225.

Rao, K., A. P. Williams, J. F. Flefil, and A. G. Konings. 2020. "SAR-Enhanced Mapping of Live Fuel Moisture Content." *Remote Sensing of Environment* 245: 111797.

Riano, D., P. Vaughan, E. Chuvieco, P. J. Zarco-Tejada, and S. L. Ustin. 2005. "Estimation of Fuel Moisture Content by Inversion of Radiative Transfer Models to Simulate Equivalent Water Thickness and Dry Matter Content: Analysis at Leaf and Canopy Level." *IEEE Transactions on Geoscience and Remote Sensing* 43, no. 4: 819–826. https://doi.org/10.1109/tgrs.2005.843316.

Roy, P. S., and P. K. Joshi. 2002. "Forest Cover Assessment in North-East India-The Potential of Temporal Wide Swath Satellite Sensor Data (IRS-1C WiFS)." *International Journal of Remote Sensing* 23, no. 22: 4881–4896. https://doi.org/10.1080/01431160110114475.

Ryan, K. C. 2002. "Dynamic Interactions Between Forest Structure and Fire Behavior in Boreal Ecosystems." *Silva Fennica* 36, no. 1: 13–39.

Schneider, P., D. A. Roberts, and P. C. Kyriakidis. 2008. "A VARI-Based Relative Greenness From MODIS Data for Computing the Fire Potential Index." *Remote Sensing of Environment* 112, no. 3: 1151–1167.

Scott, J. H., and R. E. Burgan. 2005. *Standard Fire Behavior Fuel Models: A Comprehensive Set for Use With Rothermel's Surface Fire Spread Model. General Technical Report RMRS-GTR-153*. USDA Forest Service.

Sobrino, J. A., R. Llorens, C. Fernández, J. M. Fernández-Alonso, and J. A. Vega. 2019. "Relationship Between Soil Burn Severity in Forest Fires Measured in Situ and Through Spectral Indices of Remote Detection." *Forests* 10, no. 5: 457.

Tucker, C. J. 1979. "Red and Photographic Infrared Linear Combinations for Monitoring Vegetation." *Remote Sensing of Environment* 8, no. 2: 127–150.

Viegas, D. X., M. T. S. P. Viegas, and A. D. Ferreira. 1992. "Moisture Content of Fine Forest Fuels and Fire Occurrence in Central Portugal." *International Journal of Wildland Fire* 2, no. 2: 69–86.

Wang, L., and J. J. Qu. 2007. "NMDI: A Normalized Multi-Band Drought Index for Monitoring Soil and Vegetation Moisture With Satellite Remote Sensing." *Geophysical Research Letters* 34, no. 20: L20405.

Wang, Y., X. Wei, A. D. del Campo, et al. 2019. "Juvenile Thinning Can Effectively Mitigate the Effects of Drought on Tree Growth and Water Consumption in a Young *Pinus contorta* Stand in the Interior of British Columbia, Canada." *Forest Ecology and Management* 454: 117667.

Wotton, B. M., B. J. Stocks, and D. L. Martell. 2005. "An Index for Tracking Sheltered Forest Floor Moisture Within the Canadian Forest Fire Weather Index System." *International Journal of Wildland Fire* 14, no. 2: 169–182. https://doi.org/10.1071/WF04038.

Xiao, R. 2023. "Comparison of Methods to Estimate Fuel Moisture Content in Different Forest Stand Types in Central British Columbia. Masters thesis, University of Northern British Columbia."

Yebra, M., E. Chuvieco, and D. Riaño. 2008. "Estimation of Live Fuel Moisture Content From MODIS Images for Fire Risk Assessment." *Agricultural and Forest Meteorology* 148, no. 4: 523–536. https://doi.org/10.1016/j.agrformet.2007.12.005.

Yebra, M., P. E. Dennison, E. Chuvieco, et al. 2013. "A Global Review of Remote Sensing of Live Fuel Moisture Content for Fire Danger Assessment: Moving Towards Operational Products." *Remote Sensing of Environment* 136: 455–468.

Zald, H. S., and C. J. Dunn. 2018. "Severe Fire Weather and Intensive Forest Management Increase Fire Severity in a Multi-Ownership Landscape." *Ecological Applications* 28, no. 4: 1068–1080.

Zhu, Z., C. Key, D. Ohlen, and N. Benson. 2006. *Evaluate Sensitivities of Burn-Severity Mapping Algorithms for Different Ecosystems and Fire Histories in the United States*, 35. Final Report to the Joint Fire Science Program, US Geological Survey and National Park Service.

Supporting Information

Additional supporting information can be found online in the Supporting Information section. **Figure S1:** (A) Cloud and shadow-free true colour image, and (B) NDVI for the North Fraser site, image captured on June 2nd, 2022, centred at 54.252924 N, 122.499171 W. **Figure S2:** (A) Cloudy and cloud-shadowed true colour image, and (B) NDVI for the North Fraser site, image captured on June 4th, 2022, centred at 54.252924 N, 122.499171 W. **Figure S3:** (A) Cloud true colour image, and (B) NDVI for the North Fraser site, image captured on June 9th, 2022, centred at 54.252924 N, 122.499171 W. **Figure S4:** Band value comparison between previous scene to harmonized scene in 2021 overlapping year, band data were extracted from all the clear scenes in Prince George and Smithers sample collection sites. **Figure S5:** dNBR for different stands on 6th July 2017 at Nadina, centred on 53.96890, −126.78926. **Figure S6:** Estimated duff moisture content for different stands on 6th July 2017 at Nadina, centred on 53.96890, −126.78926. **Table S1:** Table of cross-tabulation of estimated duff MC in each case study area, stand type, and burn severity category. Differences among burn severity were statistically significant ($p < 0.005$) for each fuel type, based on t test analysis. **Table S2:** Table of cross-tabulation of estimated foliage MC in each case study area, stand type, and burn severity category. Differences among burn severity were statistically significant ($p < 0.005$) for each fuel type, based on t test analysis.